

# Angular and polarization correlations in two-photon decay of hyperfine $2s$ states in hydrogenlike ions

F. Fratini<sup>1\*</sup>

<sup>1</sup> *Department of Physics, Post Office Box 3000, FI-90014, University of Oulu, Finland*

The angular and polarization properties of the photon pair emitted in the two-photon decay of  $2s$  hyperfine states in hydrogenlike ions are investigated within the relativistic Dirac framework and second order perturbation theory. The studied transitions are  $2s_{1/2} (F = 1, 0) \rightarrow 1s_{1/2} (F = 1, 0)$  in Hydrogen atom and  $2s_{1/2} (F = 4, 3) \rightarrow 1s_{1/2} (F = 4, 3)$  in hydrogenlike Uranium ion. Two different emission patterns are found: For non-spin-flip transitions, the angular correlation (*i.e.* the angular distribution of the emitted photons) is of the type  $\sim 1 + \cos^2 \theta$ , while the linear polarizations of the emitted photons are approximately parallel one another; For spin-flip transitions, the angular correlation is of the type  $\sim 1 - 1/3 \cos^2 \theta$ , while the linear polarizations of the emitted photons are approximately orthogonal one another.

PACS numbers: 31.10.+z, 32.10.Fn

## I. INTRODUCTION

The theoretical formalism of the two-photon decay in atoms and ions has been introduced by Max Born's PhD student Goepfert-Mayer in 1931 [1]. Many aspects of such a process, like the total decay rate and the spectral distribution, have been extensively investigated in the context of few-electron atoms and ions, both in theory and experiments [2–13]. Recently, some interest has been also devoted to the angular and polarization correlations of the two emitted photons [14–18], following the pioneer semi-relativistic work of Au [19]. Since the beginning of these studies, two-photon transitions in atoms and ions have been not only a challenging process to theoretically and experimentally investigate but also a useful tool with which to explore different physical areas. Already in 1940, for instance, Breit and Teller derived that the double photon emission was the principal cause of the decay of interstellar hydrogen atoms from their metastable  $2s$  state [20], while, more recently, polarization correlations of the emitted photons have been employed to successfully test violations of the Bell inequality [21–24]. Furthermore, two-photon transitions have been proposed as a tool to measure weak interaction properties [25, 26].

In the present contribution, the angular and polarization correlations of the photons emitted in two-photon decays of  $2s$  hyperfine states in hydrogenlike ions are presented. By comparing with previous theoretical results, where the two-photon decays of bare electron states in hydrogenlike ions have been analyzed, our calculations show the impact of the nuclear angular momentum (spin) on the angular and polarization properties of the emitted photons.

Nuclear features which are not easily accessible via bare nuclear physics might be successfully explored by accurately studying nuclear effects on atomic processes. A brilliant review of such effects, at the borderline between atomic and nuclear physics, has been recently written by Pálffy [27]. Along this line, owing to the significant progress that has been recently made in the development of position-sensitive photon detectors [28–31], the present paper may also outline an alternative route to probe nuclear spin properties by using two-photon transitions. The paper is structured as follows. In Sect. II the theory needed for the analysis will be explained. Particularly, in Sect. II A the states of the overall –electron plus nucleus– system will be defined. In Sect. II B, a detailed formulation of the two-photon bound–bound transition amplitude will be presented, within the framework of second order perturbation theory. Then, in Sect. II C the differential decay rate and the angular correlation of the photons will be defined in terms of the transition amplitude. In Sect. III, results for the angular correlation function, for the transitions  $2s_{1/2} (F = 1, 0) \rightarrow 1s_{1/2} (F = 1, 0)$  in Hydrogen atom as well as for  $2s_{1/2} (F = 4, 3) \rightarrow 1s_{1/2} (F = 4, 3)$  in hydrogenlike Uranium ( $^{235}_{92}\text{U}$ ) ion, will be presented and discussed. The polarization properties of the emitted radiation will be also analyzed in detail for a few of these transitions. Finally, a brief summary will be given in Sect. IV.

## II. THEORY

### A. Construction of the overall set of states

The presence of the nuclear spin has a twofold effect on the states of the overall hydrogenlike system. First, the energies of the ionic metastable states are slightly shifted, mainly due to the magnetic dipole interaction that nucleus and electron experience. This energy cor-

---

\*E-mail address: fratini@physi.uni-heidelberg.de

rection can be described by using first order perturbation theory with additional contributions, such as the relativistic, Bohr-Weisskopf, Breit-Rosenthal and QED contributions [32, 33]. Since this energy correction is too small to affect considerably the angular and polarization properties of the emitted radiation, it will be totally neglected in the following.

Secondly, the ionic states acquire a new quantum number, usually denoted by  $F$ , that represents the total angular momentum of the overall –nucleus plus electron–system. The overall ionic state can be thus described, to a first approximation, by coupling the nucleus and electron angular momenta:

$$|n, \beta; F, I, \kappa, m_F\rangle = \sum_{m_I, m_j} \langle j, m_j, I, m_I | F, m_F \rangle |n; \kappa, m_j\rangle |\beta; I, m_I\rangle, \quad (1)$$

where  $n$ ,  $\kappa$  and  $j$  are the (Bohr) principal, the Dirac and the angular momentum quantum number of the electron respectively, while  $I$  represents the nuclear spin. Finally,  $m_I$ ,  $m_j$  and  $m_F$  are the projections of the nuclear, electronic and total (nucleus plus electron) angular momentum onto the quantization axis, respectively. Using standard notation,  $\langle j, m_j, I, m_I | F, m_F \rangle$  are Clebsch-Gordan coefficients.

In writing Eq. (1), we neglected any hyperfine interaction between nucleus and electron which could, in principle, be responsible of mixing ionic states with different quantum numbers. Such a mixing could in turn affect the angular and polarization properties of the emitted radiation, which are the physical quantities we are going to investigate. Since Eq. (1) will be used in what follows, we need to estimate this approximation. We may evaluate the goodness of Eq. (1) by calculating the admixture of the state  $nS_{1/2}(F')$  that the state  $mS_{1/2}(F)$  acquires, using the non-relativistic Hamiltonian which accounts for nucleus-electron hyperfine interaction [34]:

$$\begin{aligned} \mathcal{C} &\approx k_0 \frac{8\pi}{3} \frac{\langle n, \beta; F', I, -1, m_F | \delta(\hat{r}) \hat{\mathbf{S}}\hat{\mathbf{I}} | m, \beta; F, I, -1, m_F \rangle}{E_{mS_{1/2}} - E_{nS_{1/2}}} \\ &\approx k_0 \frac{8\pi}{3} \frac{\hbar^2}{2} \frac{F(F+1) - I(I+1) - \frac{3}{4}}{E_{mS_{1/2}} - E_{nS_{1/2}}} \delta_{F,F'} \frac{Z^3}{\pi a_0^3 (nm)^{3/2}} \end{aligned} \quad (2)$$

where  $a_0$  is the Bohr radius,  $k_0 = 2g_N\mu_0\mu_B\mu_N/4\pi\hbar^2$  and  $\mu_0$ ,  $\mu_B$ ,  $\mu_N$ ,  $g_N$  are the magnetic permeability of vacuum, the Bohr magneton, the nuclear magneton and the nuclear g-factor, respectively. In the last step of the above equation, the non-relativistic values of the ionic wavefunctions at the origin together with the operator relation

$$\hat{\mathbf{S}}\hat{\mathbf{I}} = \frac{1}{2}(\hat{\mathbf{F}}^2 - \hat{\mathbf{I}}^2 - \hat{\mathbf{S}}^2) \quad (3)$$

have been used. Equation (3) is valid as long as the electron states we use are spherically symmetric, that is if they are  $s$ -states.

A property of Eq. (2) to remark is that only states with the same quantum number  $F$  can be coupled by the hyperfine interaction Hamiltonian. For  $n = 1$  and  $m = 2$ , the mixing coefficient  $\mathcal{C}$  in Eq. (2) turns out to be of order  $10^{-8}$  in Hydrogen atom while  $10^{-5}$  in hydrogenlike Uranium ion. These two numbers can be taken as estimation for the accuracy of equation (1), for the problem under consideration.

Finally, due to parity invariance of the hyperfine interaction Hamiltonian, we underline that states with different parities may not get mixed. We will discuss our results in Sect. III on the base of the considerations here presented. To further proceed, we suppose that the nucleus does not interact with the radiation field. In the language of quantum mechanics, this equates to considering that the interaction Hamiltonian couples only electron fields through photon emission, while it does not act on the quantum space of nuclear states. This hypothesis holds for decays which involve ionic bound states, since the energy released in such decays is far lower than the normal nuclear excitation energies. In contrast, in cases where the initial ionic state is a (positive) continuum–state, such hypothesis might fall as the energy of the radiation emitted in consequence of the electron capture might be enough to excite the nucleus and, therefore, to give rise to the so-called *nuclear excitation by electron capture* (NEEC) [27]. As a result of this supposition, we will find in the next subsection that the radial part of the decay amplitude will be characterized by only electron state components. Whereas, in the angular part, both the electron and nucleus states components will play a role, due to the coupling of the angular momenta.

## B. Second order transition amplitude

The theory of two–photon decay is based on the second order transition amplitude, discussed for example in Akhiezer and Berestetskii [35]. For an initial state  $|i\rangle$  and a final state  $|f\rangle$ , such amplitude reads

$$\begin{aligned} \mathcal{M}^{\lambda_1, \lambda_2}(i \rightarrow f) = & \sum_{\nu} \left[ \frac{\langle f | \vec{\alpha} \cdot \vec{u}_{\lambda_1}^* e^{-i\vec{k}_1 \cdot \vec{r}} | \nu \rangle \langle \nu | \vec{\alpha} \cdot \vec{u}_{\lambda_2}^* e^{-i\vec{k}_2 \cdot \vec{r}} | i \rangle}{E_{\nu} - E_i + \omega_2} \right. \\ & \left. + (1 \leftrightarrow 2) \right], \end{aligned} \quad (4)$$

where  $\vec{k}_j$ ,  $\vec{u}_{\lambda_j}$ ,  $\lambda_j$  and  $\omega_j$  are respectively the wave vector, the polarization vector, the helicity and the energy of the  $j$ th emitted photon ( $j = 1, 2$ ).  $E_{i, \nu}$  are the energies of the initial and intermediate ionic state, while  $\vec{\alpha}$  is the standard vector of Dirac matrices. The subscripts  $i$ ,  $\nu$ ,  $f$  will be used throughout the paper as referring to initial, intermediate and final state respectively. The summation over the intermediate states showed in formula (4) runs over the whole ionic spectrum, including a summation over the discrete part as well as an integration over the (positive and negative) continuum. For

the problem under consideration, such summation splits up into summations over the principal quantum number  $n_\nu$ , the Dirac quantum number  $\kappa_\nu$ , the total angular momentum  $F_\nu$  and its projection onto the quantization axis  $m_{F_\nu}$ .

Since the two emitted photons define generally two different trajectories, the evaluation of the angular properties of the amplitude in Eq. (4) is best carried out by decomposing the photon fields into their spherical tensor components of defined angular momentum. For the  $j$ th photon, such a decomposition reads [36]

$$\begin{aligned} \vec{u}_{\lambda_j} e^{i\vec{k}_j \cdot \vec{r}} &= \sqrt{2\pi} \sum_{L=1}^{+\infty} \sum_{M=-L}^L i^L [L]^{1/2} \left( \vec{A}_{LM}^{(m)} \right. \\ &\quad \left. + i\lambda_j \vec{A}_{LM}^{(e)} \right) D_{M\lambda_j}^L(\hat{k}_j \rightarrow \hat{z}), \end{aligned} \quad (5)$$

where  $[L] = 2L + 1$  while  $D_{M\lambda_j}^L(\hat{k}_j \rightarrow \hat{z})$  are the Wigner rotation matrices which rotate each tensor component

with angular momentum  $L$  and original quantization axis  $\hat{k}_j$  into the same component with the chosen quantization axis  $\hat{z}$ . Furthermore, the standard notation  $\vec{A}_{LM}^{(e)}$  and  $\vec{A}_{LM}^{(m)}$  is used to denote the electric and magnetic multipole, respectively. Each one of these multipoles can be expressed in terms of the spherical Bessel functions  $j_L(kr)$  and the spherical tensor  $\vec{T}_{L\Lambda M}$  as

$$\begin{aligned} \vec{A}_{LM}^{(m)} &= j_L(kr) \vec{T}_{L\Lambda M}(\hat{r}) \\ \vec{A}_{LM}^{(e)} &= j_{L-1}(kr) \sqrt{\frac{L+1}{2L+1}} \vec{T}_{L-1 M}(\hat{r}) \\ &\quad - j_{L+1}(kr) \sqrt{\frac{L}{2L+1}} \vec{T}_{L+1 M}(\hat{r}). \end{aligned} \quad (6)$$

Upon introducing Eq. (5) into (4), expanding the ionic states as showed in Eq. (1) and by taking into account that the nuclear states must be normalized, the amplitude can be written as

$$\begin{aligned} \mathcal{M}^{\lambda_1, \lambda_2}(i \rightarrow f) &= -(2\pi) \sum_{TT'} \sum_{\substack{\kappa_\nu \\ m_I m_{j\nu}}} \sum_{\substack{L_1 L_2 \\ M_1 M_2}} \sum_{p_1 p_2} \sum_{\Lambda_1 \Lambda_2} (\lambda_1)^{p_1} (\lambda_2)^{p_2} [L_1, L_2]^{1/2} i^{-L_1 - L_2 - p_1 - p_2} \xi_{L_1 \Lambda_1}^{p_1} \xi_{L_2 \Lambda_2}^{p_2} P^T P^{T'} \\ &\quad \times D_{M_2 \lambda_2}^{L_2*}(\hat{k}_2 \rightarrow \hat{z}) D_{M_1 \lambda_1}^{L_1*}(\hat{k}_1 \rightarrow \hat{z}) \left[ U_{\Lambda_1 \Lambda_2}^{TT'} \chi_{m_I m_{j\nu}}^{fT \nu T'} \chi_{m_I m_{j\nu}}^{\nu T' i T'} + (1 \leftrightarrow 2) \right], \end{aligned} \quad (7)$$

where  $\Lambda_j$  runs from  $L_j - 1$  to  $L_j + 1$ ,  $T = L, S$  is used to denote the large (L) and small (S) components of the electron Dirac spinor, for which the factor  $P^T$  is defined as  $P^L = 1$  and  $P^S = -1$ , where  $\bar{T}$  refers to the conjugate of  $T$ , *i.e.*  $\bar{T} = L$  for  $T = S$  and vice versa. Furthermore,  $p_{1,2} = 0, 1$  and the function  $\xi_{L\Lambda}^p$  is given by

$$\begin{aligned} \xi_{L\Lambda}^0 &= \delta_{L,\Lambda}, \\ \xi_{L\Lambda}^1 &= \begin{cases} \sqrt{\frac{L+1}{2L+1}} & \text{for } \Lambda = L - 1 \\ -\sqrt{\frac{L}{2L+1}} & \text{for } \Lambda = L + 1 \\ 0 & \text{otherwise} \end{cases}. \end{aligned} \quad (8)$$

The radial part of the amplitude in Eq. (7) is represented by the integral  $U_{\Lambda_1 \Lambda_2}^{TT'}$ , which reads

$$U_{\Lambda_1 \Lambda_2}^{TT'} = \int dr dr' r^2 r'^2 j_{\Lambda_1}(k_1 r') j_{\Lambda_2}(k_2 r) g_f^{\bar{T}*} g_{E_i + \omega_1}^{T \bar{T}'} g_i^{T'}, \quad (9)$$

where  $g_{f,i}^T$  are the small and large radial components of the final and initial electron state, while

$$g_{E_i + \omega_1}^{T \bar{T}'} = \sum_{n_\nu} \frac{g_\nu^T g_\nu^{\bar{T}'*}}{E_\nu - E_i - \omega_1} \quad (10)$$

is the radial Green function of the process.

By inspecting Eq. (9), we notice that the radial part of

the transition amplitude involves only electron state components. As mentioned in Sect. II A, this fact comes directly from having neglected any photon–nucleus interaction. Although the integral in Eq. (9) involves only electron state components, its evaluation is anyway a challenging task due to the (infinite) summation over the principal quantum number  $n_\nu$  contained in the radial Green function. In the present work, such integral has been computed by using the Greens library [37]. This approach has been presented for the first time in the context of two–photon decays by Surzhykov *et al.* in Ref.[14]. The angular part of the amplitude in Eq. (7) is represented by the elements  $\chi_{m_I m_{j\nu}}^{fT \nu T'}$  and  $\chi_{m_I m_{j\nu}}^{\nu T' i T'}$  therein contained and can be computed analytically. With the help of Eq. (1), we can indeed write

$$\begin{aligned} \chi_{m_I m_{j\nu}}^{fT \nu T'} &= \sum_{m_{j_f}} \langle j_f, m_{j_f}, I, m_I | F_f, m_{F_f} \rangle \\ &\quad \times \langle \kappa_f, l_f^T, m_{j_f} | \vec{\sigma} \cdot \vec{T}_{L_2 \Lambda_2 M_2}^* | \kappa_\nu, l_\nu^{\bar{T}}, m_{j_\nu} \rangle \\ \chi_{m_I m_{j\nu}}^{\nu T' i T'} &= \sum_{m_{j_i}} \langle j_i, m_{j_i}, I, m_I | F_i, m_{F_i} \rangle \\ &\quad \times \langle \kappa_\nu, l_\nu^{T'} | \vec{\sigma} \cdot \vec{T}_{L_1 \Lambda_1 M_1}^* | \kappa_i, l_i^{\bar{T}'}, m_{j_i} \rangle, \end{aligned} \quad (11)$$

where  $\vec{\sigma}$  are Pauli matrices while the elements  $\langle \kappa_f, l_f^T, m_{j_f} | \vec{\sigma} \cdot \vec{T}_{L_2 \Lambda_2 M_2}^* | \kappa_\nu, l_\nu^{\bar{T}}, m_{j_\nu} \rangle$  and  $\langle \kappa_\nu, l_\nu^{T'}, m_{j_\nu} | \vec{\sigma} \cdot$

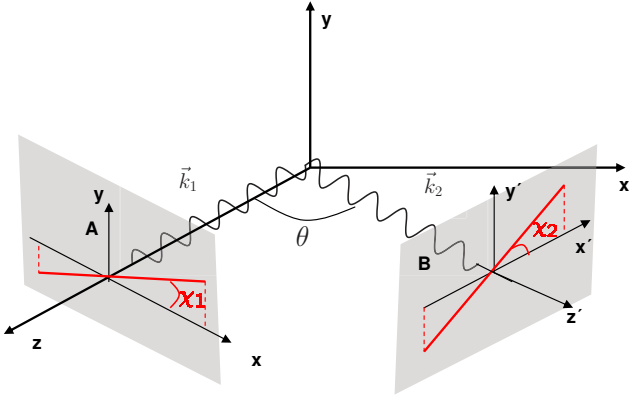


FIG. 1: (Color online) Geometry considered for the two-photon emission. The propagation direction of the first photon is adopted as  $z$  direction.  $x$  is chosen such that  $xz$  is the reaction plane (plane spanned by the two photon directions).  $\theta$  is the angle between the photons directions, while angles  $\chi_{1,2}$  define the linear polarizations of the first and second photon respectively with respect to their respective polarization planes. The polarization plane of the first (second) photon is denoted by  $A$  ( $B$ ) and represents the plane orthogonal to the photon direction.

$\vec{T}_{L_1 \Lambda_1 M_1}^* |\kappa_i, l_i^T, m_{j_i}\rangle$  have been already discussed elsewhere [14, 38] and will not be here recalled.

The initial and final states involved in the two-photon transitions which we shall analyze in Sect. III are *unpolarized*. Therefore, since for the decay of unpolarized states there is not any preferred direction for the overall system, we arbitrarily adopt the quantization axis ( $\hat{z}$ ) along the momentum of the “first” photon:  $\hat{z} \parallel \hat{k}_1$ . We furthermore adopt  $\hat{x}$  such that the  $xz$ -plane is the reaction plane (plane spanned by the photons directions). Figure 1 sketches the geometry we consider for the decay. Within this geometry, the Wigner matrices in Eq. (7) simplify to

$$\begin{aligned} D_{M_1 \lambda_1}^{L_1 *}(\hat{k}_1 \rightarrow \hat{z}) &= \delta_{M_1, \lambda_1} , \\ D_{M_2 \lambda_2}^{L_2 *}(\hat{k}_2 \rightarrow \hat{z}) &= d_{M_2 \lambda_2}^{L_2}(\theta) , \end{aligned} \quad (12)$$

where  $d_{M \lambda}^L(\theta)$  is the reduced Wigner matrix and  $\theta$  is the polar angle of the second photon, which coincides, in the chosen geometry, with the angle between the photons directions (opening angle). Hence, the relative photons directions are uniquely determined by assigning the opening angle  $\theta$ , which will be the variable against which the angular correlation will be plotted in Sect. III.

### C. Angular and Polarization correlations

Within the approximations mentioned in Sect. II A, equation (7) represents the relativistic transition amplitude for the two-photon decay between hyperfine states

in hydrogenlike ions. It contains the complete information on the emitted radiation. For instance, the energy and angle-polarization distributions of the two emitted photons can be written in terms of such transition amplitude. Assuming that the ion is initially unpolarized and that the polarization of the final ionic state remain unobserved, the differential decay rate reads (atomic units) [5]

$$\begin{aligned} \frac{dw^{\lambda_1 \lambda_2}}{d\omega_1 d\Omega_1 d\Omega_2} &= \frac{\omega_1 \omega_2}{(2\pi)^3 c^2} \frac{1}{2F_i + 1} \\ &\times \sum_{m_{F_i} m_{F_f}} \left| \mathcal{M}^{\lambda_1 \lambda_2}(i \rightarrow f) \right|^2 . \end{aligned} \quad (13)$$

By taking into account the axes geometry chosen for the two-photon emission, which has been explained in Sect. II B, we can easily perform the integration over the solid angle of the first photon ( $d\Omega_1$ ) as well as the integration over the azimuthal angle of the second photon ( $d\phi_2$ ). Now, since part of this work is devoted to analyze photons polarizations, further details concerning the detection geometry must be provided, in order to proceed with the analysis

In Fig. 1, we show how the photon polarizations may be defined in a case experiment. The polarization of each photon is to be measured in the “polarization plane”, which is the plane orthogonal to the photon direction. This means that, without loss of generality, we are considering linear (not circular) polarizations of photons. This choice is motivated by the fact that, in high energy regime, linear polarizations of photons are much more easily measured than circular polarizations. In Fig. 1, the polarization plane of the first and second photon are denoted by  $A$  and  $B$ , respectively. Each detector is supposed to have a transmission axis, along which the linear polarization of the photon is measured. Such a transmission axis is rotated by an angle  $\chi$  with respect to the reaction plane. Finally, each detector is supposed to work as a filter: Whenever a photon hits it, the detector gives off or not a “click”, which would respectively indicate that the photon has been measured as having its linear polarization along the direction  $\chi$  or  $\chi + 90^\circ$ .

By integrating over the first photon energy ( $d\omega_1$ ) and by using the well-known relations between linear and circular polarization bases [36]

$$\vec{u}_\chi = \frac{1}{\sqrt{2}} (e^{-i\chi} \vec{u}_{\lambda=+1} + e^{+i\chi} \vec{u}_{\lambda=-1}) , \quad (14)$$

we can write the differential decay rate which depends upon the photons linear polarizations as

$$\begin{aligned} W^{\chi_1 \chi_2}(\theta) &\equiv \frac{dw^{\chi_1 \chi_2}}{d \cos \theta} = \frac{8\pi^2}{2F_i + 1} \sum_{m_{F_i} m_{F_f}} \sum_{\substack{\lambda_1 \lambda_2 \\ \lambda'_1 \lambda'_2}} \\ &\times \int d\omega_1 \frac{\omega_1 \omega_2}{4(2\pi)^3 c^2} e^{i(\lambda_1 - \lambda'_1)\chi_1} e^{i(\lambda_2 - \lambda'_2)\chi_2} \\ &\times \mathcal{M}^{\lambda_1 \lambda_2} \mathcal{M}^{\lambda'_1 \lambda'_2 *}. \end{aligned} \quad (15)$$

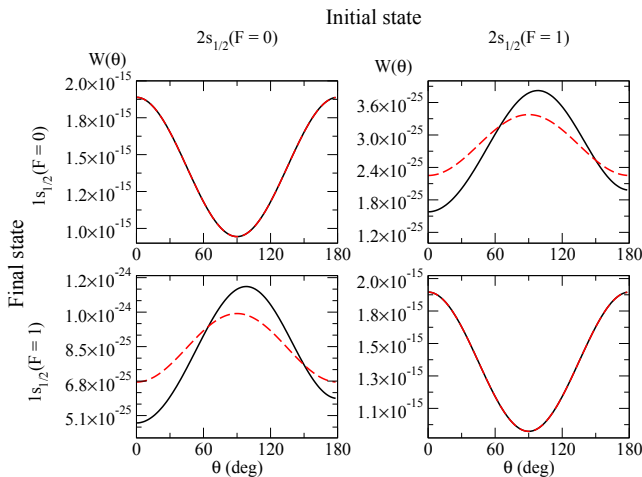


FIG. 2: (Color online) Angular correlation  $W(\theta)$  for the transitions  $2s_{1/2}(F = 1, 0) \rightarrow 1s_{1/2}(F = 1, 0)$  in Hydrogen atom. The dashed-red curve refers to the electric dipole approximation while the solid-black curve refers to the full multipole contribution.

We shall call this function “polarization correlation”. The polarization correlation represents the probability of detecting the emitted photons with defined linear polarizations  $\chi_1$  and  $\chi_2$ , in the two-photon decays of hyperfine states in hydrogenlike ions.

Finally, by summing over the photons polarizations, we define the “angular correlation” function as

$$W(\theta) \equiv \frac{dw}{d \cos \theta} = \frac{8\pi^2}{2F_i + 1} \int d\omega_1 \frac{\omega_1 \omega_2}{(2\pi)^3 c^2} \times \sum_{m_{F_i}} \sum_{m_{F_f}} \sum_{\lambda_1 \lambda_2} \left| \mathcal{M}^{\lambda_1 \lambda_2}(i \rightarrow f) \right|^2. \quad (16)$$

Equipped with equations (15) and (16), in the next section we shall investigate the functions  $W^{\chi_1 \chi_2}(\theta)$  and  $W(\theta)$  as obtained for a few decays of unpolarized hyperfine  $2s$  states in Hydrogen atom and in hydrogenlike Uranium ion.

### III. RESULTS AND DISCUSSION

In this section we shall analyze the angular and polarization correlations defined in Eqs. (15) and (16), for decays of hyperfine  $2s$  states in Hydrogen atom as well as in hydrogenlike Uranium ion.

#### A. Angular and polarization correlations in Hydrogen atom

We first analyze Hydrogen atom, whose nuclear spin is, as known,  $I = 1/2$ . In particular, we analyze the two-photon transitions  $2s_{1/2}(F = 1, 0) \rightarrow 1s_{1/2}(F =$

$1, 0)$ . The predicted angular correlation  $W(\theta)$  for these transitions is displayed in Fig. 2, where the full multipole and the electric dipole (E1E1) contributions are separately displayed. We might immediately notice that, in the two transitions  $2s_{1/2}(F = 1) \rightarrow 1s_{1/2}(F = 1)$  and  $2s_{1/2}(F = 0) \rightarrow 1s_{1/2}(F = 0)$ , the curves obtained within the electric dipole approximation practically coincide with the curves obtained with the full multipole contribution. The angular correlation in these transitions can be well described by  $W(\theta) \sim 1 + \cos^2 \theta$ , which is *symmetric* with respect to  $\theta = 90^\circ$  and which is the analytical form that has been for long associated to the angular correlation in  $2s \rightarrow 1s$  two-photon transitions in Hydrogenlike bound systems [11, 19, 39].

Whereas, the radiation patterns in  $2s_{1/2}(F = 1) \rightarrow 1s_{1/2}(F = 0)$  and  $2s_{1/2}(F = 0) \rightarrow 1s_{1/2}(F = 1)$  transitions show a different, *asymmetric* shape. It can be seen that high-multipole contributions are directly responsible for the asymmetry, while the contribution of the leading E1E1 multipole can be well described by  $W_{E1E1}(\theta) \sim 1 - 1/3 \cos^2 \theta$ . This result is typical for two-photon decays of the type  $J_{TOT} = 1(0) \rightarrow J_{TOT} = 0(1)$ , where  $J_{TOT}$  is the total angular momentum of the system which undergoes the decay. In fact the two-photon decay  $(1s 2s)^3 S_{J=1} \rightarrow (1s 1s)^1 S_{J=0}$  in heliumlike ions, where  $J$  is the total angular momentum of the system given by the coupling of the two electron angular momenta, shows approximately the same behavior [17, 40]. Quantitatively, the asymmetry

$$\mathcal{A} = \frac{W(\theta = 180^\circ) - W(\theta = 0^\circ)}{W(\theta = 180^\circ)} \quad (17)$$

is approximately 0.20 in  $F = 1(0) \rightarrow F = 0(1)$  transitions, while it is vanishing in  $F = 1(0) \rightarrow F = 1(0)$  transitions.

Difficulties in measuring the correlation function in those transitions where the total spin ( $F$ ) is flipped ( $F = 0(1) \rightarrow F = 1(0)$ ) might arise from the fact that the decay rates for these transitions are noticeably nine orders of magnitude smaller than the decay rates for the transitions in which the spin is not flipped ( $F = 0(1) \rightarrow F = 0(1)$ ), as seen from Fig. 2. This fact is caused by the strong cancellation of the contributions given by the  $p_{1/2}$  and  $p_{3/2}$  intermediate states (in the calculation of the leading multipole E1E1) to the correlation function in  $F = 0(1) \rightarrow F = 1(0)$  transitions. As a matter of fact, within non-relativistic dipole approximation, these two contributions are equal and opposite, so that the transitions  $2s_{1/2}(F = 1) \rightarrow 1s_{1/2}(F = 0)$  and  $2s_{1/2}(F = 0) \rightarrow 1s_{1/2}(F = 1)$  cannot proceed via two-photon dipole E1E1 emission [17, 41]. Thus, the non-vanishing correlation functions showed in the top-right and bottom-left panels of Fig. 2 are only given by high-multipole and relativistic effects.

As a consequence of what said above, any experimental incoherent population of the initial and final hyperfine states would result in measuring the angular correlation function as given by  $\sim 1 + \cos^2 \theta$ . This has been con-



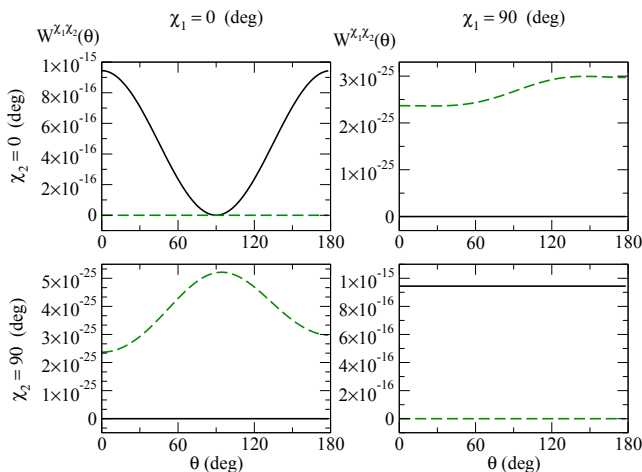


FIG. 3: (Color online) Polarization correlation  $W^{\chi_1 \chi_2}(\theta)$  for the transitions  $2s_{1/2}(F=0) \rightarrow 1s_{1/2}(F=0)$  (solid-black curve) and  $2s_{1/2}(F=0) \rightarrow 1s_{1/2}(F=1)$  (dashed-green curve) in Hydrogen atom. The four polarization configurations ( $\chi_1, \chi_2 = 0^\circ, 90^\circ$ ) are separately displayed.

firm, for example, in Refs. [42, 43]. For a direct experimental investigation of the angular correlation function in  $F=1(0) \rightarrow F=0(1)$  transitions, one would therefore normally need to selectively populate the initial and observe the final hyperfine state. Such a selection could be made, in principle, by resolving energetically the emitted photons. The two hyperfine states  $2s(F=1)$  and  $2s(F=0)$ , as well as the states  $1s(F=1)$  and  $1s(F=0)$ , although they have been considered degenerate in the present paper, possess in fact slightly different energies due to the well-known hyperfine energy splitting, which is of the order  $\sim 10^{-6}$  eV in both cases (see Sect. II A). However, the energy resolution of normal photon detectors for light quanta in the visible range, which is the energy range of the photons emitted in the considered transitions, is far lower than  $10^{-6}$  eV. Therefore, the selection of initial and final hyperfine states cannot proceed by analyzing energy.

Alternatively, in order to achieve the same goal, we could make use of the linear polarization properties of the emitted photons. In Fig. 3, we plot the polarization correlation  $W^{\chi_1 \chi_2}(\theta)$  as obtained for the transitions  $2s_{1/2}(F=0) \rightarrow 1s_{1/2}(F=0)$  and  $2s_{1/2}(F=0) \rightarrow 1s_{1/2}(F=1)$  in Hydrogen atom. As it can be seen, the orthogonal linear polarization configurations  $\chi_1 = 0^\circ, \chi_2 = 90^\circ$  and  $\chi_1 = 90^\circ, \chi_2 = 0^\circ$  are absent in  $F=0 \rightarrow F=0$  transition. More quantitatively, from Fig. 3 we can identify the photons' polarization state for  $F=0 \rightarrow F=0$  transition as being

$$|\Psi\rangle = \frac{1}{\sqrt{1 - \cos^2 \theta}} \left( |\chi_1 = 0, \chi_2 = 0\rangle + e^{i\delta} \cos \theta |\chi_1 = 90^\circ, \chi_2 = 90^\circ\rangle \right), \quad (18)$$

where the phase  $\delta$  can be determined, for instance, by analyzing the polarization correlation in the helicity basis. By doing that, one easily finds  $\delta = 0$ . Although not directly shown, the photons polarization state in Eq. (18) holds also in case the photons came from  $F=1 \rightarrow F=1$  transition.

In Refs. [18, 24], the same photons polarization state has been derived by analyzing  $2s \rightarrow 1s$  transitions in hydrogenlike ions within non-relativistic dipole approximation and without considering the nuclear spin. This is consistent with what found above, since, as mentioned,  $F=0(1) \rightarrow F=1(0)$  transitions are forbidden within non-relativistic dipole approximation and therefore the polarization state displayed in Eq. (18) is the only one which the photons can assume in two-photon  $2s \rightarrow 1s$  transitions.

Coming back to Fig. 3, we notice that the decay rate for orthogonal polarization configurations is not vanishing for  $F=0 \rightarrow F=1$  transition, for any angle  $\theta$ , although its order of magnitude is very small in comparison with the decay rates shown in other panels of the same figure. This fact allows us to suggest a workable scenario for investigating the angular and polarization correlations in two-photon  $F=0 \rightarrow F=1$  transitions. By using standard devices of modern spectroscopy, we can experimentally exclusively populate the initial  $2s_{1/2}(F=0)$  state [44]. Such a state would consequently decay either into  $1s_{1/2}(F=0)$  or  $1s_{1/2}(F=1)$  state. Now, as already underlined, only the transition  $2s_{1/2}(F=0) \rightarrow 1s_{1/2}(F=1)$  of the two is characterized by non-vanishing decay rate for two photons having orthogonal linear polarizations. Thus, we could select out the two-photon decay channel  $F=0 \rightarrow F=1$  just by filtering the photons polarizations. By virtue of the fact that the wavelength of each emitted quanta in this decay is roughly  $\approx 250$  nm and that polarizer crystals are available in such wavelength range, we could place one linear polarizer filter in front of each photon detector. We would use the detectors in coincidence and we would set opposite linear polarizers transmission axes of the filters, in order to allow only the photon pairs coming from  $2s_{1/2}(F=0) \rightarrow 1s_{1/2}(F=1)$  transition to be detected. By inspecting the orders of magnitude of the decay rates in Fig. 3, we notice that, in order to successfully block the unwanted light from  $F=0 \rightarrow F=0$  transition, the extinction ratio of the polarizers must be higher than  $10^{10}:1$ . Such performances should be achievable by using in series, for instance, two or more normal polarizers whose extinction ratio is usually of order  $10^5:1$ . Problems related to the alignment of the polarizers might however arise.

By using this sketched set-up, we should therefore be sensible only to those photons that come from  $2s_{1/2}(F=0) \rightarrow 1s_{1/2}(F=1)$  transition and that have the selected polarization configuration, *i.e.* we will measure the dashed-green curve showed either in the bottom-left or in the top-right panel of Fig. 3, depending on the polarizers settings.

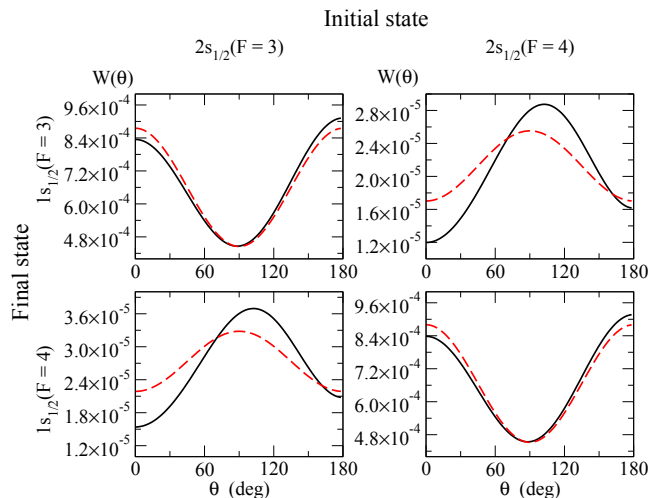


FIG. 4: (Color online) Angular correlation  $W(\theta)$  for the transitions  $2s_{1/2}(F = 4, 3) \rightarrow 1s_{1/2}(F = 4, 3)$  in hydrogenlike  $^{235}\text{U}$ . The dashed-red curve refers to the electric dipole approximation while the solid-black curve refers to the full multipole contribution.

Due to the intrinsic weakness of the signal coming from the desired decay channel, one could at this point think that the hyperfine interaction itself, here neglected from the outset, may mix states with different quantum numbers, so that the angular and polarization properties of the emitted radiation could vary from what shown in Figs. 2 and 3. However, as briefly discussed in Sect. II A, the Hamiltonian which accounts for the hyperfine interaction neither mixes states with different parities nor  $S$ -states with different quantum number  $F$ . This implies that the state  $2s_{1/2}(F = 0)$  does not acquire any admixture of any other state and thus remains well defined. Indeed low energy hyperfine states in Hydrogen atom are known to be well separated, as it is evident from the fact that the light emitted in the hyperfine transition of  $1s_{1/2}$  state in Hydrogen is one of the most accurately measured physical quantities ever and is of great importance in astrophysics and cosmology.

### B. Angular and polarization correlations in hydrogenlike Uranium

We proceed to analyze hydrogenlike  $^{235}\text{U}$  ion, whose nuclear spin is  $I = 7/2$  [45]. In particular, we study the transitions  $2s_{1/2}(F = 4, 3) \rightarrow 1s_{1/2}(F = 4, 3)$  in such ion. Hydrogenlike heavy ions are interesting bound systems both from a theoretical and an experimental point of view, since they are as simple as Hydrogen atom but show, at the same time, remarkable relativistic and high-multipole effects. We have nonetheless seen that high-multipole effects show already up in  $F = 0(1) \rightarrow F = 1(0)$  transitions in Hydrogen atom, where they are directly responsible for the asymmetric behaviour of the angular

correlation function (cfr. Fig. 2). In  $^{235}\text{U}$  ion, we expect an enhancement of this effect.

The angular correlation,  $W(\theta)$ , of the photon pair for  $2s_{1/2}(F = 4, 3) \rightarrow 1s_{1/2}(F = 4, 3)$  two-photon transitions in hydrogenlike  $^{235}\text{U}$  ion is displayed in Fig. 4. The full multipole and the electric dipole (E1E1) contributions are separately displayed. Although the spin properties of  $^{235}\text{U}$  and  $^1\text{H}$  are considerably different, we can see that the relative (photon) angular correlations are rather similar in shape. However, by inspecting carefully both Figs. 4 and 2, it can be noticed that, as expected, high-multipole effects play overall a more important role in  $^{235}\text{U}$  than in Hydrogen. First, in contrast to Hydrogen, the angular correlation for non-spin-flip transitions ( $F = 3(4) \rightarrow F = 3(4)$ ) show sizable deviations from the  $\sim 1 + \cos^2\theta$  shape. This effect is already known from the past literature, where it has been showed that high multipoles contribute with terms of the type  $\sim \cos\theta$  to the angular correlation in  $2s_{1/2} \rightarrow 1s_{1/2}$  transitions [19]. Secondly, we also notice that, in spin-flip transitions ( $F = 3(4) \rightarrow F = 4(3)$ ), deviations of the angular correlation function from the symmetric analytical formula  $\sim 1 - 1/3 \cos^2\theta$  are more pronounced in hydrogenlike  $^{235}\text{U}$  ion than in Hydrogen. More concretely, for the case of  $^{235}\text{U}$  ion, the asymmetry  $\mathcal{A}$  defined in Eq. (17) turns out to be approximately 0.26 in  $2s_{1/2}(F = 4(3)) \rightarrow 1s_{1/2}(F = 3(4))$  transitions, while it is 0.09 in  $2s_{1/2}(F = 4(3)) \rightarrow 1s_{1/2}(F = 4(3))$  transitions.

It can be furthermore noticed that each one of the  $2s \rightarrow 1s$  two-photon transitions shown in Fig. 4 is characterized by far higher decay rate with respect to the transitions shown in Fig. 2. This fact is not surprising since it is known that the total decay rate for this transition rises fast with  $Z$ , as it can be approximately expressed by  $\sigma \approx 8.226 Z^6 \text{ sec}^{-1}$  [2].

As a final remark, by comparing Figs. 4 and 2, we notice that spin-flip transitions are less suppressed in hydrogenlike Uranium than in Hydrogen atom, which is a consequence of the fact that relativistic and retardation effects characterize highly charged ions. The selective detection of the photon pair coming from  $F = 3(4) \rightarrow F = 4(3)$  transitions in hydrogenlike Uranium, however, is complicated by the fact that the energy of the emitted radiation is in the range of hard X-rays. The discernment by energy analysis of the decay channels in  $^{235}\text{U}$  share the same problem already encountered in the Hydrogen case: The hyperfine energy splitting between  $2s_{1/2}(F = 4)$  and  $2s_{1/2}(F = 3)$ , as well as the one between  $1s_{1/2}(F = 4)$  and  $1s_{1/2}(F = 3)$ , is of the order  $\sim 1 \text{ eV}$ , which is far smaller than the normal resolution of X-ray detectors. In addition, since there exist no polarizer filters for such energy regime, the photon polarization analysis suggested to select the desired decay channel in the Hydrogen case is not immediately applicable to Uranium, regardless of the polarization properties of the emitted photons. As a matter of fact, the polarization resolved experiments in X-ray energy regimes are not normally performed by

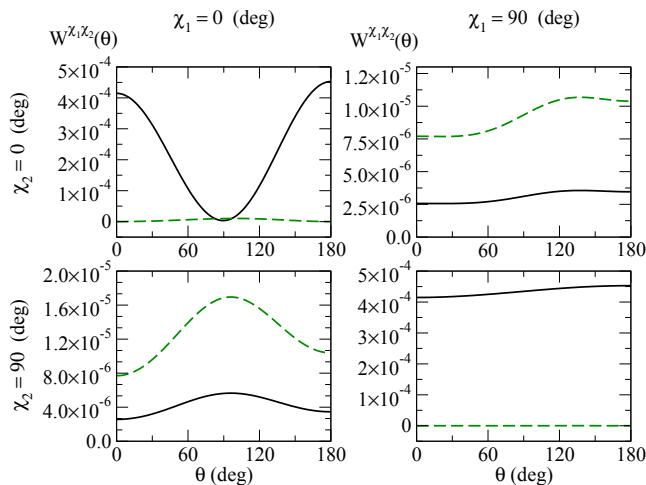


FIG. 5: (Color online) Polarization correlation  $W^{\chi_1 \chi_2}(\theta)$  for the transitions  $2s_{1/2}(F=3) \rightarrow 1s_{1/2}(F=3)$  (solid-black curve) and  $2s_{1/2}(F=3) \rightarrow 1s_{1/2}(F=4)$  (dashed-green curve) in hydrogenlike  $^{235}\text{U}$  ion. The four polarization configurations ( $\chi_1, \chi_2 = 0^\circ, 90^\circ$ ) are separately displayed.

using polarizer filters, but rather by using Compton polarimeters [28–30, 46, 47]. In such devices, the information about the photon polarization is obtained from the reconstruction of the Compton scattering events (of the incident photons) in the detector and thus has a statistical nature. As a consequence, Compton polarimeters are not normally used to record the polarization properties in multi-photon processes. Rather, they are employed to record the polarization properties in single photon processes [31]. Nonetheless, by selecting events which have been recorded in coincidence by two or more Compton polarimeters and which have the desired scattering angle, information on the polarization of a multi-photon state could be in principle achieved [26, 48–51].

In the light of such possibility, we present in Fig. 5 the function  $W^{\chi_1 \chi_2}(\theta)$  as obtained for the transitions  $2s_{1/2}(F=3) \rightarrow 1s_{1/2}(F=3)$  and  $2s_{1/2}(F=3) \rightarrow 1s_{1/2}(F=4)$  in hydrogenlike  $^{235}\text{U}$  ion. We see from the figure that the general scheme for which photons coming from spin-flip transitions (non-spin flip transitions) have mainly orthogonal (parallel) linear polarizations remains valid also in hydrogenlike Uranium. However, in

the Uranium case, the suppressed polarization configurations are more evident, especially in spin-flip transitions, where they turn out to be of the same order of magnitude of the leading polarization configurations. Thus, in contrast to Hydrogen, there exist not any polarization configuration by which to single out the photons coming from one transition of the two displayed in Fig. 5.

#### IV. SUMMARY

In summary, the angular and polarization correlations in two-photon decays of  $2s$  hyperfine states in hydrogenlike ions have been investigated within second-order perturbation theory and the Dirac relativistic framework. Results for the angular correlation have been showed for the transitions  $2s_{1/2}(F=1,0) \rightarrow 1s_{1/2}(F=1,0)$  in Hydrogen atom as well as for  $2s_{1/2}(F=4,3) \rightarrow 1s_{1/2}(F=4,3)$  in hydrogenlike  $^{235}\text{U}$  ion. It has been possible to identify two types of emission pattern: 1- the two-photon decays which connect ionic states with the same spin (non-spin-flip transitions) are found to be characterized by an angular correlation  $W(\theta) \sim 1 + \cos^2 \theta$ , with small deviations which are increasing with the atomic number  $Z$ ; 2- the two-photon decays which connect ionic states with different spin (spin-flip transitions) are found to have much smaller decay rate and to be characterized by an angular correlation  $W(\theta) \sim 1 - 1/3 \cos^2 \theta$ , with deviations which are already important for low- $Z$  systems. In both cases, the (asymmetric) deviations come from high-multipole contributions.

Results for the polarization correlation have been showed for the transitions  $2s_{1/2}(F=0) \rightarrow 1s_{1/2}(F=1,0)$  in Hydrogen as well as for  $2s_{1/2}(F=3) \rightarrow 1s_{1/2}(F=4,3)$  in hydrogenlike  $^{235}\text{U}$  ion. It has been found that the photons coming from the studied  $F=0 \rightarrow F=0$  transition in Hydrogen atom are exclusively characterized by parallel linear polarization. By using such results, it has been possible to outline a way to experimentally measure the angular and polarization correlations in the transition  $2s_{1/2}(F=0) \rightarrow 1s_{1/2}(F=1)$ , in Hydrogen atom.

#### Acknowledgments

The author acknowledges Prof. R.B. Thayyullathil for his suggestions.

[1] M. Goeppert-Mayer, Ann. Phys. (Leipzig) **9**, 273 (1931).  
 [2] J. Shapiro and G. Breit, Phys. Rev. **113**, 179 (1959).  
 [3] G. W. F. Drake and S. P. Goldman, Phys. Rev. A **23**, 2093 (1981).  
 [4] G. W. F. Drake, Phys. Rev. A **34**, 2871 (1986).  
 [5] S. P. Goldman and G. W. F. Drake, Phys. Rev. A **24**, 183 (1981).  
 [6] A. Derevianko and W. R. Johnson, Phys. Rev. A **56**, 1288 (1997).

[7] J. P. Santos, F. Parente, and P. Indelicato, Eur. Phys. J. D **3**, 43 (1998).  
 [8] R. W. Dunford, H. G. Berry, S. Cheng, E. P. Kanter, C. Kurtz, B. J. Zabransky, A. E. Livingston, L. J. Curtis, Phys. Rev. A **48**, 1929 (1993).  
 [9] R. Ali, I. Ahmad, R. W. Dunford, D. S. Gemmill, M. Jung, E. P. Kanter, P. H. Mokler, H. G. Berry, A. E. Livingston, S. Cheng, and L. J. Curtis, Phys. Rev. A **55**, 994 (1997).



- [10] H. W. Schäffer, P. H. Mokler, R. W. Dunford, C. Kozhuharov, A. Krämer, A. E. Livingston, T. Ludziejewski, H. T. Prinz, P. Rymuza, L. Sarkadi, Z. Stachura, Th. Stöhlker, P. Swiat, and A. Warczak, *Phys. Lett. A* **260**, 489 (1999).
- [11] P. H. Mokler and R. W. Dunford, *Phys. Scr.* **69**, C1 (2004).
- [12] A. Kumar, S. Trotsenko, A. V. Volotka, D. Banaś, H. F. Beyer, H. Bräuning, A. Gumberidze, S. Hagmann, S. Hess, C. Kozhuharov, R. Reuschl, U. Spillmann, M. Trassinelli, G. Weber, and Th. Stöhlker, *Eur. Phys. J. Special Topics* **169**, 19 (2009).
- [13] S. Trotsenko, *et al.*, *Phys. Rev. Lett.* **104**, 033001 (2010).
- [14] A. Surzhykov, P. Koval and S. Fritzsche, *Phys. Rev. A* **71**, 022509 (2005).
- [15] L. Borowska, A. Surzhykov, Th. Stöhlker and S. Fritzsche, *Phys. Rev. A* **74**, 062516 (2006).
- [16] A. Surzhykov, T. Radtke, P. Indelicato and S. Fritzsche, *Eur. J. Phys. Special Topics* **169**, 29-34 (2009).
- [17] A. Surzhykov, A. Volotka, F. Fratini, J. P. Santos, P. Indelicato, S. Fritzsche and Th. Stöhlker, *Phys. Rev. A* **81**, 042510 (2010).
- [18] F. Fratini and A. Surzhykov, *Hyp. Int.* **199**, 85 (2011).
- [19] C. K. Au, *Phys. Rev. A* **14**, 531 (1976).
- [20] G. Breit and E. Teller, *Astrophys. J.* **91**, 215 (1940).
- [21] A. Aspect, J. Dalibard, and G. Roger, *Phys. Rev. Lett.* **49**, 1804 (1982).
- [22] W. Perrie, A. J. Duncan, H. J. Beyer, H. Kleinpoppen, *Phys. Rev. Lett.* **54**, 1790 (1985).
- [23] H. Kleinpoppen, A. J. Duncan, H. J. Beyer, and Z. A. Sheikh, *Phys. Scr.* **T72**, 7 (1997).
- [24] F. Fratini, M. C. Tichy, Th. Jahrsetz, A. Buchleitner, S. Fritzsche and A. Surzhykov, *Phys. Rev. A* **83**, 032506 (2011).
- [25] A. Schäfer, G. Soff, P. Indelicato, B. Müller and W. Greiner, *Phys. Rev. A* **40**, 7362 (1989).
- [26] F. Fratini, S. Trotsenko, S. Tashenov, Th. Stöhlker and A. Surzhykov, *Phys. Rev. A* **83**, 052505 (2011).
- [27] A. Pálffy, *Cont. Phys.* **51**, 471 (2010).
- [28] U. Spillmann, H. Bräuning, S. Hess, H. Beyer, Th. Stöhlker, J. C. Dousse, D. Protic and T. Krings, *Review of Scientific Instruments* **79**, 083101 (pages 8) (2008).
- [29] G. Weber, H. Bräuning, S. Hess, R. Martin, U. Spillmann and Th. Stöhlker, *Journal of Instrumentation* **5**, C07010 (2010).
- [30] P. S. Shaw, U. Arp, A. Henins and S. Southworth, *Rev. Sci. Instrum.* **67**, 3362 (1996).
- [31] S. Tashenov, Th. Stöhlker, *et al.*, *Phys. Rev. Lett.* **97**, 223202 (2006).
- [32] V. M. Shabaev, M. Tomaselli, T. Kühl, A. N. Artemyev and V. A. Yerokhin, *Phys. Rev. A* **56**, 252 (1997).
- [33] S. G. Karshenboim and V. G. Ivanov, *Phys. Lett. B* **524**, 259 (2002).
- [34] B. H. Bransden, C. J. Joachain, *Physics of Atoms and Molecules* (Longman, New York, 1983).
- [35] A. I. Akhiezer and V. B. Berestetskii, *Quantum Electrodynamics* (Wiley, New York, 1965).
- [36] M. E. Rose, *Elementary Theory of Angular Momentum* (Wiley, New York, 1953).
- [37] P. Koval and S. Fritzsche, *Comp. Phys. Commun.* **152**, 191 (2003).
- [38] A. Surzhykov, S. Fritzsche and Th. Stöhlker, *J. Phys. B* **35**, 3713 (2002).
- [39] S. Klarsfeld, *Phys. Lett.* **30A**, 382 (1969).
- [40] P. H. Mokler and R. W. Dunford, *Phys. Scr.* **69**, C19 (2004).
- [41] K. D. Bonin and Th. J. McIlrath, *J. Opt. Soc. Am. B* **1**, 52 (1984).
- [42] M. Lipeles, R. Novick and N. Tolk, *Phys. Rev. Lett.* **15**, 690 (1965).
- [43] D. O'Connell, K. J. Kollath, A. J. Duncan and H. Kleinpoppen, *J. Phys. B* **8**, L214 (1975).
- [44] N. E. Rothery and E. A. Hessels, *Phys. Rev. A* **61**, 044501 (2000).
- [45] N. J. Stone, *Atomic Data and Nuclear Tables* **90**, 75-176 (2005).
- [46] D. Protic, E. L. Hull, T. Krings, and K. Vetter, *IEEE Transactions on Nuclear Science* **52**, 3181 (2005).
- [47] D. Protic, Th. Stöhlker, T. Krings, I. Mohos, and U. Spillmann, *IEEE Transactions on Nuclear Science* **52**, 3194 (2005).
- [48] M. H. L. Pryce and J. C. Ward, *Nature* **160**, 435 (1947).
- [49] H. S. Snyder, S. Pasternack and J. Hornbostel, *Phys. Rev.* **73**, 1398 (1948).
- [50] C. S. Wu and I. Shakhov, *Phys. Rev.* **77**, 136 (1950).
- [51] E. Bleuler and H. L. Brandt, *Phys. Rev.* **73**, 1398 (1948).